1st International Conference on Science and Technology Innovation (ICoSTEC)
February, 26 2022. Yogyakarta, Indonesia
ISBN: 978-623-331-338-4

MODELLING AND ANALYSIS OF PVSC TYPE BUCK BUCK-BOOST DC-DC CONVERTER

T Ram Manohar Reddy[1], Shaik Hussain Vali[2], Phanindra Thota[3], Kamaraju V[4]

[1,2]*Department of Electrical and Electronics Engineering, College of Engineering (A), Pulivendula, JNTU Anantapur*

[3,4]*Department of Electrical Engineering, AU College of Engineering (A), Visakhapatnam-530003*

[1]rammanoharreddy793@gmail.com

[2]hussianvali4@gmail.com

[3]phanindras.thota@gmail.com

[4]raju.vechalapu@gmail.com

***Abstract*— In the era of modern industrial development, power electronics equipment has been developed aggressively and brought dc system again in power utilization to use clean energy resources like solar array, fuel cell, wind generator, etc. Since the past decade, power electronics equipment has become very popular; hence, the switch-mode converter requirement is increasing rapidly day by day in applications like communication power supply, space crafts, hybrid electric vehicles, micro-grid and nano-grids. Among the various available configurations of converters, Multi-Input DC/DC converters became more and more popular in power electronics field, especially, for provide interface of various renewable energy sources and deliver regulated power to several loads. In this article, a PVSC type Buck Buck-Boost Dual-Input DC- DC Converter (DIDC) is designed and modelled for DC grid application. The proposed converter is driven with two renewable energy sources PV cell and a battery having different amplitudes which can able to deliver the power from source to load individually or simultaneously. DIDC tropology is simply configured with two passive elements L, C, diodes D_1 D_2 and switches S_1, S_2. The Dual-Input DC-DC Converter suitability is validated by carrying out simulations in different modes of operation. The de-centralized PID controller is designed for voltage and current loop controller to ensure the DC output voltage of 48 V, load current of 4.8 A and power of 230W. The Stability of the closed-loop converter is also verified under all possible source and load disturbance conditions. The simulations and analysis of the proposed converter are carried out using MATLAB and PSIM software**

***Keywords*— dc-dc converter, controller, modelling, dc grid, power electronics**

I. INTRODUCTION

The power demand is increasing globally, due to increase of power utilities due to urbanization. To meet the ever-increasing power demand consumers are approaching towards the clean energy. The power generation from renewables are mostly intermittent in nature especially solar and wind. Standalone use of these source may lead to uninterrupted in power supply to utility. So, integration of different sources as input to the utilities helps to improve the reliability. Multi input topologies are introduced to overcome the de merits of each single input topologies. Nowadays, Multi-Input DC-DC converters became more and more popular in power electrics field especially for hey provide interface of various renewable energy sources and deliver regulated power to several loads. In most power electronic systems, input power, output demand, or both instantaneously change and are not exactly identical with each other at any time instant. Hence, providing a good match between them is a complicated task to deal with if not impossible. Furthermore, due to the wide variation of processed power, overall efficiency of the system is not high. Hence, additional energy sources are required to assist the main source in fulfilling the load demand.

Multi-Input DC-DC converter for hybrid energy system are proposed in [1]. In [2] Systematic approach of various multi-input DC-DC topologies are presented. In [3] Numerous multi-input topologies for renewable applications are reviewed. A non-isolated high gain multi-input topology is proposed in [4]. A single switch boost-buck DC-DC topology for industrial applications is proposed in [5]. Selection of non-isolated DC-DC topology for PV systems is surveyed in [6]. A non-isolated DC-DC boost topology is proposed in [7]. A modified non-isolated DC-DC topology is prosed for PV application in [8]. Multi-input single-output non-isolated DC-DC topology for PV systems in [9]. Modular non-isolated high step-up multi-input DC-DC topology is proposed in [10].

The synthesis of multi-input converters are broadly classified in to two categories viz. (i) Pulsating Voltage Source Cell (PVSC) type and (ii) Pulsating Current Source Cell (PCSC) type (Li et al., 2010). The converter topology considered in this paper is a PVSC type Buck Buck-Boost Dual-Input DC-DC converter (DIDC). Section-II presents the modelling of DIDC converter. Section-III, presents the results obtained from various case studies using the developed DIDC model and at the end conclusions are furnished in section-IV.

II. MODELLING OF DIDC CONVERTER

The proposed DIDC converter consists of two input sources V_{g1}, V_{g2}, two switches S_1&S_2, two passive elements inductor (L) and capacitor (C) and a restive load R shown in Figure-1

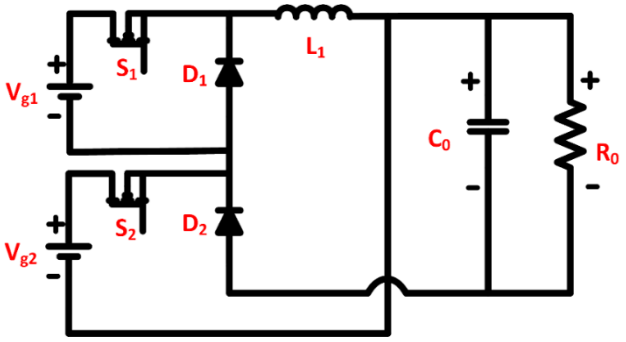

Fig. 1 Dual-Input DC-DC Converter

A) Principle of operation

The DIDC configuration is non-isolated type and it can able to deliver the power to load in single conversion stage with the two voltage sources by simultaneous ON and OFF of the power switches S_1 and S_2 with their respective duty ratios d_1 and d_2. During the ON/OFF of switches the passive elements in the circuit charges and discharges for a specific time period T_s. During ON time the elements in the converter are get charges and in OFF time it is discharges through load. The operating of the converter depends on the ON/OFF sequences of the power switches with their corresponding duty cycles d_1 and d_2. The modes of operation of DIDC topology for a switch period T_s is shown in Fig. 1 switching time interval of Mode-I is d_2T_s, switching time interval of Mode-II is $(d_1\text{-}d_2)T_s$ and switching time interval of Mode-III is $(1\text{-}d_2)T_s$.

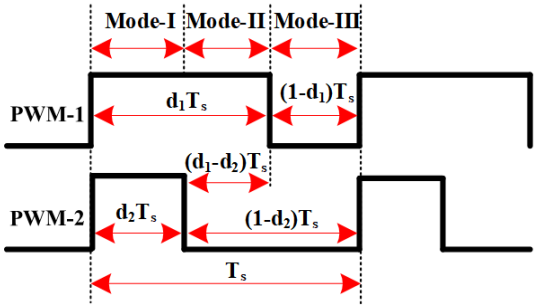

Fig. 1 Switching Sequence of Different Operating Modes of DIDC

1) Operating Mode-I: In this mode of operation, the two switches S_1 and S_2 are in turned-on condition and the diodes D_1 and D_2 are in turned-off condition. The Inductor L_1 is charged by the two voltage sources V_{g1} and V_{g2}. The equivalent circuit for mode-1 operation is shown in Fig. 3. The inductor voltages and capacitor currents represent the dynamics of this converter are obtained by applying Kirchhoff's laws the rate of change in voltage and currents of the elements w.r.t time are expressed in equations (1) & (2).

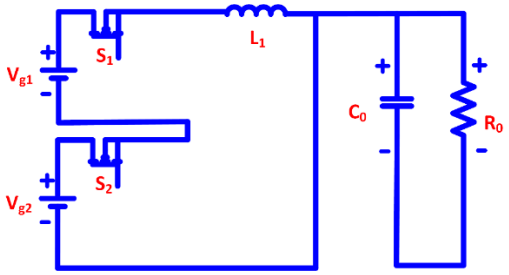

Fig. 3 Operating Mode-I

$$V_{g1} + V_{g2} = V_L \tag{1}$$

$$i_{co} = \frac{-VC_0}{R_0} \tag{2}$$

2) Operating Mode-II: In this mode of operation, the switch S_1 and diode D_2 are in turned-on condition and the diodes D_1 and switch S_2 are in turned-off position. In this mode of operation, voltage V_{g1} the Inductor L_1 and drives the load R_0. The equivalent circuit for mode-2 operation is shown in Fig. 4

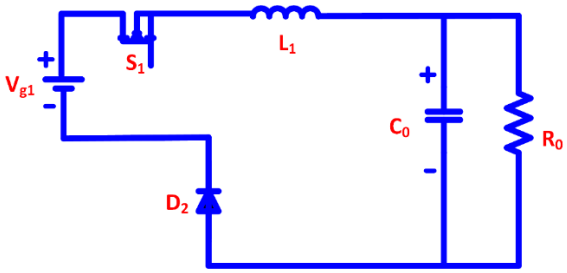

Fig. 4 Operating Mode-II

By applting Kirchhoff's laws to the operating mode-II voltage across the inductor and current through capacitors are given in equations (3) and (4).

$$V_{g1} + V_L = V_{c0} \tag{3}$$

$$i_{co} = i_L \frac{-V_{c0}}{R_0} \tag{4}$$

$$V_0 = V_{c0} \tag{5}$$

3) Operating Mode-III: In this mode of operation, the two switches S_1 and S_2 are in turned-on condition and the two diodes D_1 and D_2 in turned-off position. In this mode of operation Inductor L_1 discharges through the load R_0. The equivalent circuit for mode-3 operation is shown in Fig .5. By applying Kirchhoff's laws to this operating mode voltage across the inductor and current through capacitors are given in equations (6) & (7).

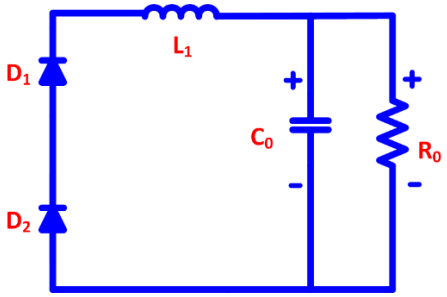

Fig. 5 Operating Mode-III

$$V_L = V_{c0} \quad (6)$$

$$V_0 = V_{c0} \quad (7)$$

The voltages across the inductos, status of the inductors, active sources and switches of the DIDC during three modes of operation is given in Table I.

TABLE I
DIFFERENT MODES OF OPERATION OF THE DIDC

Operating Modes	Mode-I	Mode-II	Mode-III
Active Sources	$V_{g1} + V_{g2}$	V_{g1}	None
Active Switches	S_1, S_2	S_1, D_2	D_1, D_2
Status of Inductor	Charging	Charging	Discharging
Voltage across the inductor	$V_{g1}+V_{g2}$	$V_{g1}-V_{c0}$	V_{c0}

B) Steady state condition:

In steady state condition the average voltage across of the converter as per the volt-sec balance principle is zero.

$$\int_0^{Ts} V_L = 0$$

Average voltage across the inductor V_L over a switching cycle of T_s. The output voltage of DIDC is obtained by applying the volt-sec to the inductor given in Table-I obtained from the different modes of operations is

$$V_0 = (V_{g1}-2V_{C0})d_1 + V_{g1}d_2 + (1+V_{C0})d_2$$

The output voltage of given in equation (6) variation with respective duty ratios d_1 and d_2 are plotted in Fig. 6. The range of duty cycles are chosen as $0 \le d_1 \le 0.6$ and $0 \le d_2 \le 0.4$. The variation in output voltage of the DIDC converter will reach up to approximately 260 V for the chose range of duty cycles.

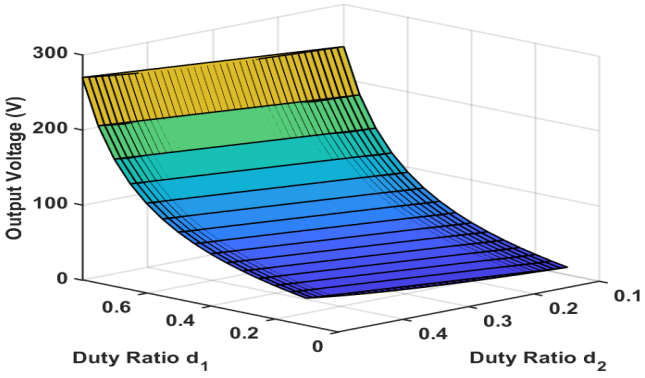

Fig. 6 D-plot for output voltage variation with d_1 and d_2

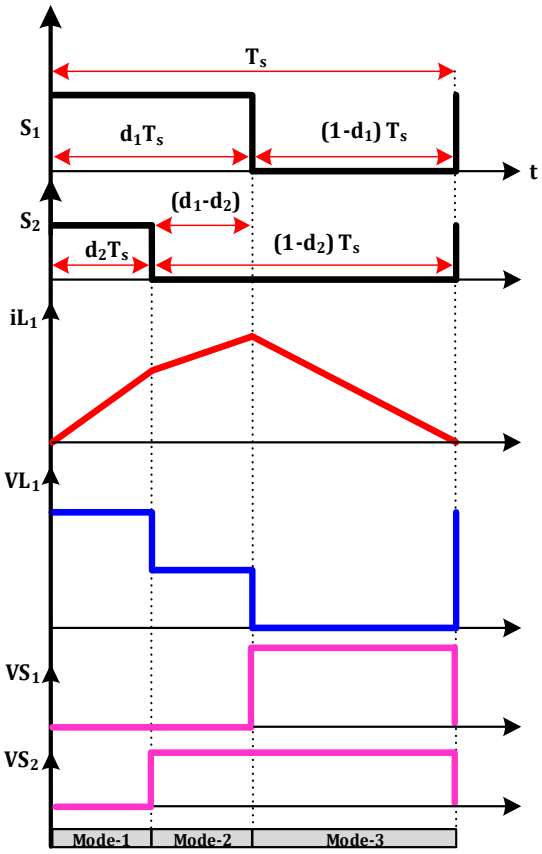

Fig. 7 Steady state waveforms of DIDC

III. RESULTS AND DISCUSSION

A) Simulation Results

A 230 W, 48 V DIDC model is simulated using PSIM and parameters considered for the simulation are given in Table-II. The duty ratios and output voltage and inductor current of DIDC in open loop simulation is shown in Figures 7 & 8.

TABLE II
PARAMETERS OF THE CONVERTER

Parameter	Value
Inductor L1	300 μH
Capacitor C0	200 μF
Voltage Source V_{g1}	60 V
Voltage Source V_{g2}	30 V
Resistor	10 Ω
Duty Cycle d_1	0.42
Duty Cycle d_2	0.295
Switching Frequency	50 Khz

In open loop condition DIDC is operating with nominal parameters i.e. nominal condition, but in practical scenarios converter input source and loads may get deviated due to fluctuations and increase/decrease in load. The deviations from the normal condition affects the efficiency of the system. To overcome these dynamic conditions a closed-loop PID controller is designed for DIDC topology. The topology is having two controlling inputs (d_1, d_2) and two controllable outputs v_0 and i_L therefore, two controllers designed for DIDC. The PID values of both the controllers are listed in Table-III

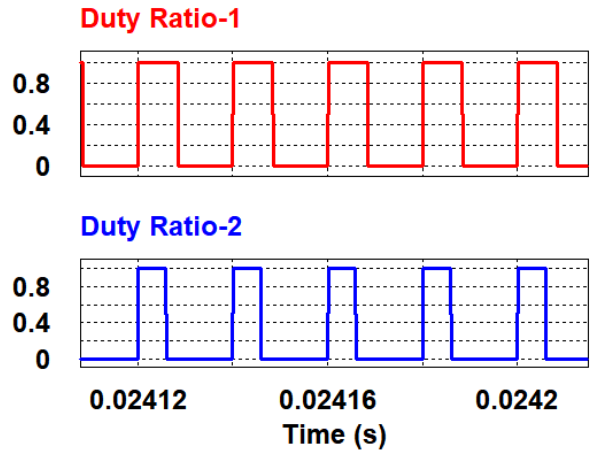

Fig. 7 Duty ratios

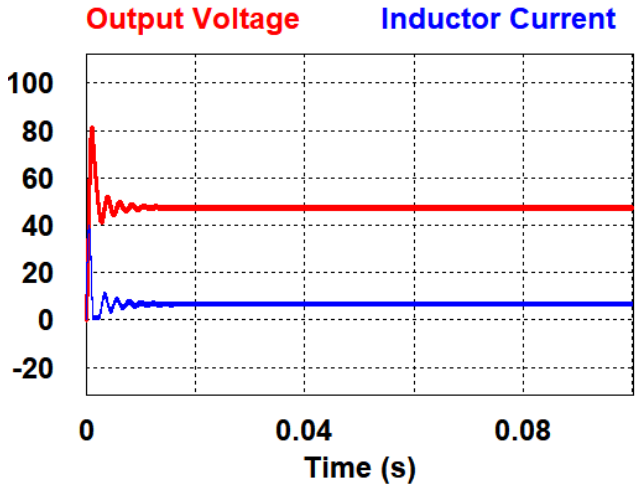

Fig. 7 Open loop simulation of DIDC

TABLE II
PID CONTROLLERS

Controller	P	I	D
V_0	0.0125	0.943	0.979
iL	0.3104	0.957	0.9897

To verify the closed-loop stability using PID controller few dynamic cases were considered. The output voltage V_0 and inductor current i_L in nominal operating condition is $V_0 = 48V$ & $i_L = 5.1$ A.

1) Case-i: In this case the source V_{g1} is deviated from 40 V to 70 V. The incremental in amplitude of the source V_{g1} at 40 msec over a time period of 1 msec and observe that the output voltage is increased up to 52 V and the inductor current remains same shown in Fig.8.

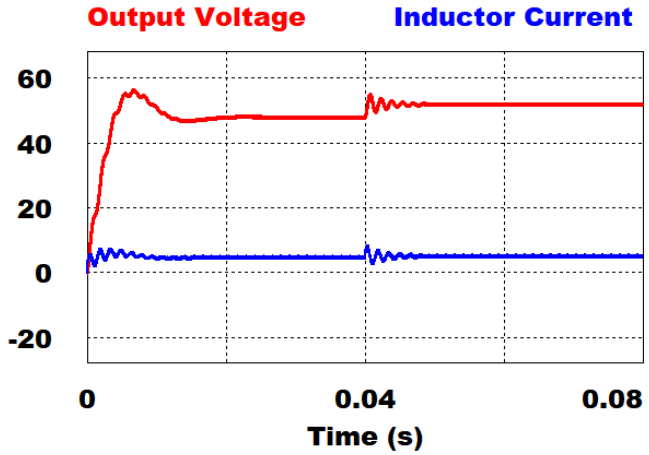

Fig. 8 Output voltage and inductor current of DIDC when V_{g1} is incremented

2) Case-ii: In this case load dynamics are considered, at initial time period the load on the converter is 6 ohms, 4 ohms load is further added to the initial 6 ohms of load resistance at 70 msec. The inductor current is increased to 8A and output voltage remains same shown in Fig. 9.

3) Case-iii: In this case the source voltage sources V_{g1} and V_{g2} is incremented to 70 V and 40 V from its nominal voltages 60 V and 30 V. The incremental in amplitude of both the voltages 40 msec over a time period of 1 mesc. Load dynamics are considered for the same case, at initial time period the load on the converter is 6 ohms, 4 ohms load is further added to the initial 6 ohms of load resistance at 70 msec. The observation from this case is whenever voltage sources are incremented the output load voltage is increased from 48 V to 52 V and inductor current is unchanged at 40 msec. The current in the inductor is increased to 5.6 A and further increased to 9.4 A when load is added at 70 msec and the output voltage is 52 V same at 40 msec. shown in Fig. 10.

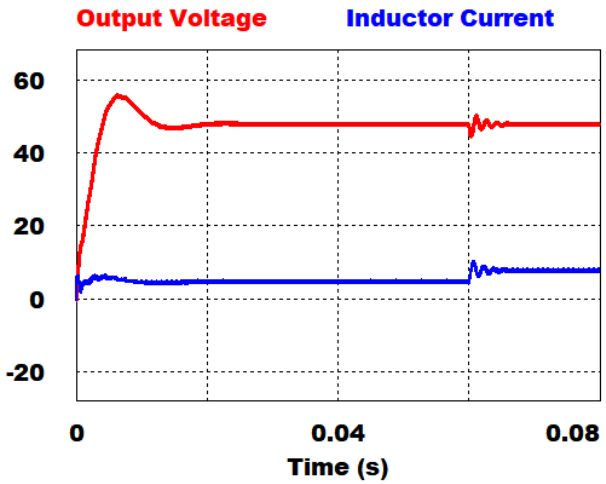

Fig. 8 Output voltage and inductor current of DIDC when R is incremented.

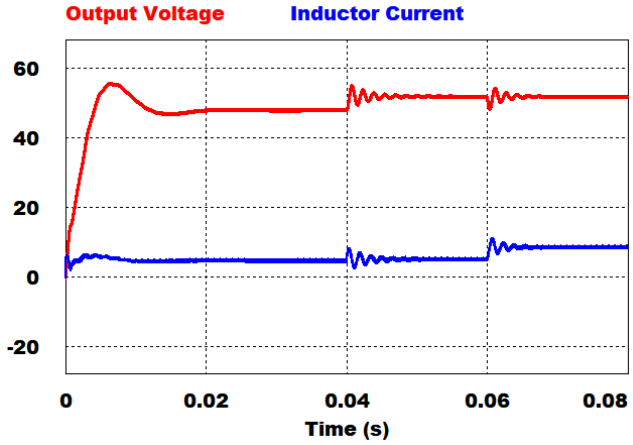

Fig. 9 Output voltage and inductor current of DIDC when both V_{g1}, V_{g2} and R is incremented.

4) Case-iv: In this case the source voltage source V_{g1} is decremented to 55 V from nominal voltage 60 V similarly, V_{g2} is also decremented to 18 V from 30 V. The decremental amplitude of both the voltages of the converter at 40 msec over a time period of 1 msec. Load dynamics are considered for the same as in case-iii, observation from this case is whenever the decrement of voltages V_{g1} and V_{g2} the output load voltage is dropped from 48 V to 43V. The inductor current is 4.4 A at 40 msec, and it is further increased to 7.2 A when the load is added at 70 msec. shown in Fig. 11.

From the above cases it is clearly observed that PID controller is stabilizing the dynamic conditions of DIDC under closed-loop operation with in a less tine i.e. less than 0.02 msec. Hence, the designed PID controller restoring the disturbance with in a less time and achieving stability.

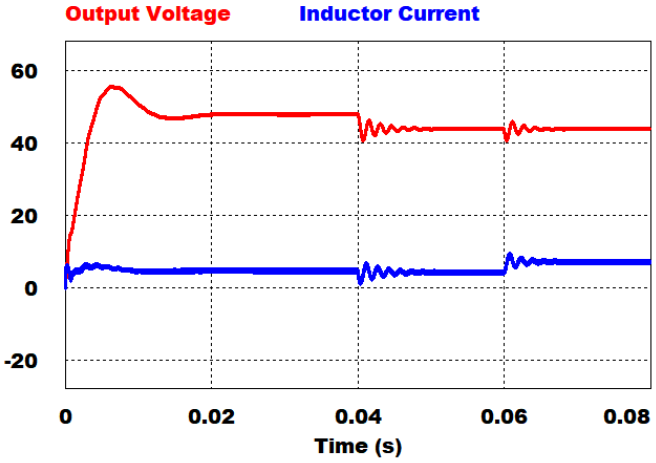

Fig. 11 Output voltage and inductor current of DIDC when both V_{g1}, V_{g2} and R is decremented.

IV. CONCLUSION

A new DIDC topology suitable for integration of two renewable energy sources is presented in this paper. Different operating modes of the topology are analysed and then a digital PID controller is designed. The performance and stability of the DIDC is studied for various dynamic conditions. Simulation results shown that under all dynamic condition cases the designed PID controller is performing well and achieving stability within less time after to the disturbance.

REFERENCES

[1] Kumar, Lalit, and Shailendra Jain. "Multiple-input DC/DC converter topology for hybrid energy system." IET Power Electronics 6, no. 8 (2013): 1483-1501.

[2] Liu, Yuan-Chuan, and Yaow-Ming Chen. "A systematic approach to synthesizing multi-input DC–DC converters." IEEE Transactions on Power Electronics 24, no. 1 (2009): 116-127.

[3] Rehman, Zubair, Ibrahim Al-Bahadly, and Subhas Mukhopadhyay. "Multiinput DC–DC converters in renewable energy applications–An overview." Renewable and Sustainable Energy Reviews 41 (2015): 521-539.

[4] Zhang, Hao, Jiao Gao, Xiaojin Wan, and Fang Liu. "Bifurcation-Based Dynamical Stability and Coupling Analysis of Dual-Input Buck-Boost DC–DC Converters." International Journal of Bifurcation and Chaos 32, no. 01 (2022): 2250012.

[5] Dhimish, Mahmoud, and Nigel Schofield. "Single-switch boost-buck DC-DC converter for industrial fuel cell and photovoltaics applications." International Journal of Hydrogen Energy 47, no. 2 (2022): 1241-1255.

[6] Singh, S. N. "Selection of non-isolated DC-DC converters for solar photovoltaic system." Renewable and Sustainable Energy Reviews 76 (2017): 1230-1247.

[7] Shayeghi, Hossein, Saeed Pourjafar, Mohammad Maalandish, and Soheil Nouri. "Non-isolated DC–DC converter with a high-voltage conversion ratio." IET Power Electronics 13, no. 16 (2020): 3797-3806.

[8] Saravanan, Subramani, and Neelakandan Ramesh Babu. "A modified high step-up non-isolated DC-DC converter for PV application." Journal of applied research and technology 15, no. 3 (2017): 242-249.

[9] Banaei, Mohammad Reza, Hossein Ardi, Rana Alizadeh, and Amir Farakhor. "Non-isolated multi-input–single-output DC/DC converter for photovoltaic power generation systems." IET Power Electronics 7, no. 11 (2014): 2806-2816.

[10] Varesi, Kazem, Seyed Hossein Hosseini, Mehran Sabahi, and Ebrahim Babaei. "Modular non-isolated multi-input high step-up dc–dc converter with reduced normalised voltage stress and component count." IET Power electronics 11, no. 6 (2018): 1092-1100.